Svedberg Open
DISSEMINATION OF KNOWLEDGE

International Journal of Artificial Intelligence and Machine Learning

Publisher's Home Page: https://www.svedbergopen.com/

Research Paper Open Access

Webcam-Based Detection of Visual Ocular Impairments Based on Opacity, Shape, Ring Appearance and Position Using Media-Pipe Face Mesh For Accessibility-Aware Web Personalization

Amar Ranjan Dash[1*], Manas Ranjan Patra[2]

[1*]PhD Scholar, Computer Science Department, Berhampur University, Berhampur, INDIA. Email: amarnath_9876@yahoo.co.in
[2]Professor, CSE Department, NIST University. Pallur Hills, Berhampur, INDIA. Email: mrpatra@nist.edu

ABSTRACT

Visual impairments caused by ocular abnormalities can directly affect a user's ability to perceive and interact with digital content. The standard eye examination normally relies on specialized imaging equipment and professional experience. This paper proposes a non-invasive, webcam-based framework. It detect visually observable ocular impairments and generate personalized accessible web-interface. The RGB video captured from a regular laptop webcam is processed with Media-Pipe Face Mesh, which is used to identify facial landmarks as well as eye and iris landmarks and pupils, before going through the visual analysis of the disease. The proposed framework is based on four complementary approaches to detecting ocular abnormalities: position-based, opacity-based, shape-based, and appearance-based analysis using rings. The modules cover the following 7 target conditions: squint, cataract, sclerocornea, corneal scarring, corneal ulcer, iris coloboma and Arcus Senilis. Scale-normalized ocular measurements are employed to reduce sensitivity to variations in user-to-camera distance and head orientation. The extracted features are integrated into a unified impairment profile. Thisse profiles subsequently mapped to personalized accessibility adaptations such as text enlargement, contrast enhancement, magnification, spacing optimization, and simplified interaction. Evaluation on a 1,000-sample test dataset produced an overall classification accuracy of 98.20%. The model demonstrate the feasibility of the proposed approach for webcam-based ocular-condition screening. The framework also offers a means for integrating ophthalmic impairment assessment with adaptive human–computer interaction while eliminating the need for dedicated ophthalmic imaging equipment.

Keywords: Visual Impairment Detection, Webcam-Based Screening, Media Pipe Face Mesh, Anterior Eye Disease Detection, Ocular Feature Analysis, Accessibility-Aware Web Personalization, Adaptive Human–Computer Interaction

1. INTRODUCTION

The process of essay evaluation has traditionally been labor-intensive, subjective, and time-consuming, Visual impairment can substantially influence how users perceive and interact with digital information. Web accessibility guidelines offer some general guidelines for improving the accessibility and usability of web pages. Traditional accessibility mechanisms are known to implement pre-defined interface adaptations. But they are not capable to respond to the specific visual characteristics of individual users. Thus, users with different ocular limitations may encounter similar interfaces despite having substantially different perceptual requirements.

The advancements in computer vision and AI have facilitated computer-assisted assessment of the eye based on images of the face, eye, fundus, near-infrared eye, slit-lamp and optical coherence tomography. Most existing approaches are designed for clinical diagnosis and depend on specialized imaging devices or controlled acquisition conditions. These requirements restrict their deployment in everyday computing environments.

The proposed study addresses this gap through a unified framework. The Framework detect visually observable ocular impairments from RGB images and videos captured using a standard laptop webcam. Media-Pipe Face Mesh is used to localize facial and ocular landmarks, eye contours, iris boundaries, and pupil centers. Based on the predominant visual expression, the framework groups detection into four complementary categories. Position-based analysis identifies squint through pupil alignment and relative ocular geometry. In opacity-based analysis, the pupil and corneal regions are characterized by their intensity and structural features, to classify cataract, sclerocornea, corneal scarring and corneal ulcer. Shape-based analysis detects iris coloboma through pupil-contour characteristics. Ring-appearance-based analysis identifies Arcus Senilis using normalized peripheral corneal-ring features.

Direct measurements of the pixels are unstable as the distance, head pose and viewing orientation of the user affects the acquisition of the webcam. Hence, in the framework, landmark normalization and relative measurements are used to enhance the consistency of features. In particular, normalized ocular geometry is used for pupil-shape analysis and peripheral ring measurements.

The framework not only detects the impairment but also contains an accessibility recommendation engine that translates the detected ocular profile into individual changes to the interface, such as enlarging text, boosting the contrast, zooming, spacing, simplifying layouts, and providing navigation assistance. A dataset of 1,000 webcam video samples covering seven ocular conditions and a normal-eye class was constructed for evaluation. The proposed system achieved 98.20% overall classification accuracy, demonstrating the feasibility of webcam-based multi-condition ocular screening and accessibility-aware personalization.

The principal contributions are a unified webcam-based ocular screening framework, disease-specific analysis using position, opacity, shape, and ring-appearance. It also Proposes a mechanism that links ocular assessment with personalized web-interface adaptation.

2. Literature Review

With the recent development of artificial intelligence (AI), computer vision, and deep learning, the screening of ocular disorders has now been greatly resculpted by automating the analysis of facial, ocular, retinal, and fundus images. Most diagnosis of ophthalmic disorders is done through special clinical diagnostics and by qualified health care professionals, and is therefore not accessible to everyone, especially in remote and resource-limited areas. Thus, there has been a growing interest in the study of image-based computational approaches to the identification of abnormalities in the eyes, from anatomical deformities to abnormalities in visual function. Existing studies can generally be grouped according to the impairment visual characteristics such as position abnormalities, geometric variations, structural changes, opacity formation and functional vision deficiencies.

2.1. Geometrical Position based impairedness detection

The spatial location of the components of the eye, especially the gaze orientation and eye alignment, is important for diagnosis of disorders, including strabismus. The detection of strabismus using automatic computer vision-based screening systems has received significant attention because of the possibility of performing the screening process quickly and noninvasively. Yarkheir et al. **Error! Unknown switch argument.** developed a deep learning architecture for automatic detection and classification of strabismus from facial images, suggesting that it is possible to extract the features of the eye alignment directly from the facial images. In an effort to address this challenge, Wu et al. **Error! Unknown switch argument.** developed an artificial intelligence (AI)-driven screening system using the Vision Transformer (ViT) architecture to aid in clinical management and the detection of strabismus on a large scale. The use of image-based screening in remote health care applications is also evident in the work of Kurdthongmee et al. **Error! Unknown switch argument.** where a telemedicine-oriented strabismus detection approach based on monocular eye images was developed. By combining deep learning models with a user-friendly diagnostic system, Joshi **Error! Unknown switch argument.** proposed a convolutional neural network (CNN)-based graphical user interface for automated squint classification. Karaaslan et al **Error! Unknown switch argument.** presented a method using image processing and the Hirschberg test together with Support Vector Machine (SVM) classification to determine the ocular deviations with higher reliability. While these methods show good results, most current systems are developed specifically for clinical applications and require controlled image acquisition conditions. But their use in general purpose webcam based accessibility systems is relatively unexplored. In this regard, dash et al. **Error! Unknown switch argument.** came up with a machine learning based computer vision (CV) solution that could detect and classify twelve types of squint present in real-time video streams.

2.2. Geometrical Shape based impairedness detection

The structure of the eye, including its iris, cornea and abnormal tissue growth can be used as a good indicator of eye related disorder. The automatic analysis of eye geometry has developed to a large extent from iris recognition, where accurate iris segmentation and feature extraction are crucial. Adegoke et al. **Error! Unknown switch argument.** gave a thorough survey of the iris segmentation algorithms, emphasizing the significance of precise localization of the iris boundaries in order to enable accurate eye analysis. Liu et al. **Error! Unknown switch argument.** studied indicators of ophthalmic linked to endocrine disorders, focusing on the diagnostic potential of the structural changes detected in different parts of the eye. Daugman **Error! Unknown switch argument.** enhanced the robustness of iris recognition systems by making a number of improvements, such as the use of an active contour approach for segmenting the iris, the use of flexible coordinate modeling, the enhancement of process for handling gaze axis, and improved score normalisation techniques.

There have been recent investigations on the extension of the above ocular shape analysis to abnormality detection. To detect iris coloboma from retinal fundus images, Pratibha et al. **Error! Unknown switch argument.** presented an artificial intelligence (AI) framework using Vision Transformers and Explainable AI (XAI). Armstrong et al. **Error! Unknown switch argument.** studied a very unusual clinical case of bilateral ocular coloboma in relationship to a deletion of the maternally inherited RARB gene, showing how structural abnormalities of the eyes can also be highly complex and genetically associated.

One of the main areas of shape-based research in the eye has been in the area of Arcus Senilis detection, in that the lipid deposit in the periphery of the cornea will change the appearance of the iris–corneal region. Ramlee et al. **Error! Unknown switch argument.** and **Error! Unknown switch argument.** successfully showed that existing iris recognition pipelines (localization, segmentation, normalization, and feature extraction) can be applied to non-invasive screening for cholesterol levels from anterior eye photographs. Another improvement to Arcus Senilis detection was introduced by Songire et al. **Error! Unknown switch argument.** and Bhangdiya **Error! Unknown switch argument.** which added Circular Hough Transform-based iris segmentation, histogram analysis and handcrafted feature extraction techniques.

As machine learning technology progresses, researchers have moved from handcrafted features to automatically learning features. To differentiate healthy eye, Arcus Senilis and Arcus Senilis in cataract condition, SV et al. **Error! Unknown switch argument.** created a Computer Aided Diagnosis (CAD) system based on segmentation methods and Support Vector Machine (SVM) classification. Amini et al. **Error! Unknown switch argument.** have used the concept of transfer learning with the AlexNet to automatically learn discriminative features of the eyes that do not need to be handcrafted.

Despite these advances, current shape-based impairment detection methods mainly focus on higher resolution near-eye images taken under controlled conditions. Their requirement for a special imaging setup renders them unsuitable for low-cost, webcam-based accessibility applications.

2.3. Opacity Based-Disorder Detection

Opacity formation within ocular structures, particularly the lens and cornea, is one of the major causes of visual impairment. Automated detection of opacity-related disorders such as cataract, corneal scarring, and corneal ulceration has therefore become an important research area in ophthalmic image analysis. Unlike geometric abnormalities, opacity-based disorders are primarily characterized by variations in transparency, texture, and light transmission properties of ocular tissues.

Various studies have explored the automatic detection of cataract from the fundus image, the anterior eye image and the retinal image. Automated diagnosis using deep learning models was shown by Yang et al. **Error! Unknown switch argument.** who proposed a neural network-based retinal image classification framework for cataract screening. The use of CNN-based methods for cataract detection from fundus images was further studied by Junayed et al. **Error! Unknown switch argument.**, Khan et al. **Error! Unknown switch argument.** and Wu et al. **Error! Unknown switch argument.** who investigated ResNet-50 architectures and multi-task learning techniques. These techniques achieved better classification performance using high level features extracted automatically from the image, which correlate with lens opacity. Tripathi et al. **Error! Unknown switch argument.** suggested a multi-task learning framework for the segmentation of the Iris and the Pupil from near infrared (NIR) eye images, for the purpose of cataract assessment. Likewise, Ganokratanaa et al. **Error! Unknown switch argument.** studied a LeNet based CNN for the identification of cataract images where they showed that the lightweight deep learning architecture is capable of successfully detecting an eye disease.

In addition to lens opacity, high-resolution imaging of the eye has also been studied to look at abnormalities in the sclera and cornea. The research efforts in this area, however, have mainly been directed toward the visualization and the structural evaluation of the eye rather than towards the automatic detection of the eye diseases, like sclerocornea. Anterior Segment Optical Coherence Tomography (AS-OCT) has become a standard imaging tool for assessing anterior ocular structures such as the cornea, limbus, sclera, trabecular meshwork and Schlemm's canal. Gupta et al. **Error! Unknown switch argument.** analyzed the clinical utility of AS-OCT in the assessment of corneal disease and Rollins et al. **Error! Unknown switch argument.** and Radhakrishnan et al. **Error! Unknown switch argument.** showed its potential for high-resolution and real-time imaging of the anterior segment. Ueno et al. **Error! Unknown switch argument.** enhanced the visualization of the cornea using polarization-sensitive OCT, and Lombardo et al. **Error! Unknown switch argument.** combined AS-OCT with microscopic imaging for detailed corneal analysis.

Specialized imaging systems have also been used for the assessment of corneal scars. In order to improve the visualisation of scarred corneal tissues on AS-OCT, Girard et al. **Error! Unknown switch argument.** proposed an algorithm called Corneal Adaptive Compensation. In vivo confocal microscopy and quantitative image analysis were used by Simpson et al. **Error! Unknown switch argument.** to evaluate the pathological changes in corneas and progress of scars. Cree and Jelinek et al. **Error! Unknown switch argument.** emphasized the crucial role of image quality and acquisition parameters in the enhancement of the reliability of automated corneal lesion detection.

Recent studies have also developed the use of deep learning approaches for automated detection and grading of corneal ulcers. In order to localize corneal ulcer, Qasmieh et al. **Error! Unknown switch argument.** fused the conventional image processing techniques and ResNet18-based semantic segmentation. In order to segment the corneas and classify the ulcers, Manawongsakul et al. **Error! Unknown switch argument.** proposed an integrated framework by implementing the CNN and U-Net architecture for the image segmentation of corneas and ulcers simultaneously, as well as for ulcer severity grading. Over the last years, Alakuş and Baykara **Error! Unknown switch argument.** investigated the use of Vision Transformer (ViT) for ulcer classification and severity assessment, showcasing the rise of transformer models in ophthalmic image analysis.

While these methods have yielded much clinical diagnostic improvement, the majority of opacity detection systems rely on slit-lamp imaging, OCT, fundus imaging or other specialized ophthalmic devices. However, their direct application in low cost webcam based screening and accessibility based application is still a challenge.

2.4. Accessibility-Oriented Ocular Analytics

While conventional ophthalmic research primarily focuses on disease diagnosis, recent studies have explored the integration of artificial intelligence with accessibility technologies to create adaptive human-computer interaction systems.

These approaches seek to comprehend the visual capacities of individuals and adjust digital spaces as a result. Herath et al. **Error! Unknown switch argument.** proposed an artificial intelligence based multi-modal system for monitoring the health of the eyes, visual fatigue and disease screening, using webcam based eye tracking and deep learning techniques. Their findings showed that continuous ocular evaluation was possible with consumer grade cameras.

Kartynnik et al. **Error! Unknown switch argument.** presented a novel, real-time monocular framework for facial landmark detection (FLD) which was later expanded into MediaPipe Face Mesh. This technology allows to extract the facial and ocular landmarks with high accuracy from standard RGB cameras, thereby providing opportunities for low-cost analysis of the geometry of the eye without using specialized hardware.

Previous studies have primarily considered the accessibility issues in terms of adherence to accessibility standards. Patra et al. **Error! Unknown switch argument.**,**Error! Unknown switch argument.** investigated Web Content Accessibility Guidelines (WCAG) compliance across government and institutional websites. In addition, Patra and Dash **Error! Unknown switch argument.**,**Error! Unknown switch argument.** conducted a study on accessibility features of web browsers and multimedia platforms in desktop and mobile platforms.

While these studies contribute to digital access, they are mostly based on generic accessibility requirements and not based on customisation of the interface based on the specific visual impairments. Thus, real-time detection of ocular impairment coupled with adaptive Web personalization is a significant new research trend.

2.5. Research Gap

According to the literature reviewed, great advances have been made in the field of automated detection of ocular disorders through the application of artificial intelligence and computer vision. The current methods, however, are mostly designed for the clinical diagnosis of targeted eye diseases with retinal images, fundus photos, OCT, slit-lamp images, and other specialized ophthalmic imaging modalities.

Most of the existing systems are directed towards the detection of single disorders like cataract, abnormalities related to glaucoma, corneal lesions, strabismus, or retinal diseases. These methods are highly accurate diagnostic techniques, but are not easily applicable in a typical computing environment, due to the need for expensive imaging hardware.

Moreover, much of the current research on digital accessibility focuses on assessing compliance to standards like WCAG or on analysing assistive technologies but not on the visual properties of the users as they are when using the technology. Typical accessibility solutions are based on the universal design paradigm and offer an identical interface to all users, regardless of the type of visual impairment.

A significant research opportunity therefore exists in developing a low-cost, webcam-based framework capable of identifying visual ocular impairments through easily observable characteristics such as ocular position, structural shape, opacity variations, ring appearance, pupil behaviour, visual acuity, and colour perception. To address this limitation, the present study proposes a computer vision-based ocular impairment detection framework using Media-Pipe facial landmark analysis and image-based feature extraction techniques. The proposed system identifies visual impairments based on four major categories: Opacity-based abnormalities, Shape-based abnormalities, Ring appearance variations, and Position-based abnormalities. The extracted impairment profile is subsequently utilized to enable adaptive web personalization, providing a user-specific accessibility mechanism rather than a generalized one-size-fits-all approach.

The remainder of this paper is organized as follows: Section 3 introduces the concept of opacity, shape, ring, and position-based visual impairments. Section 4 describes the proposed visual impairment detection methodology. Section 5 presents experimental results, performance analysis, and comparison with existing approaches. Finally, Section 6 concludes the paper and discusses future research directions.

3. Background on Visual Impairedness

Visual impairment is a reduction in visual function caused by congenital abnormalities, age-related degeneration, trauma, or ocular diseases affecting different anatomical structures of the eye. Although some eye diseases need to be diagnosed with specialized clinical imaging, a few anterior eye diseases cause distinct changes in eye appearance that can be seen with standard RGB cameras. The visual signs are corneal opacity or lens opacity, abnormalities of the iris, peripheral corneal rings and misalignment of the eyes. Such observable characteristics provide an opportunity to develop non-invasive webcam-based screening systems using computer vision techniques. The ocular conditions included in this study can be grouped into four classes, based on their visual characteristics: opacity-based, shape-based, ring appearance based, and position-based. These classifications are consistent with the proposed feature extraction framework which involves the analysis of disease-specific visual features, prior to classification.

3.1. Opacity Based

Opacity-based ocular disorders are characterized by partial or complete loss of transparency within the optical media of the eye. Under normal conditions, the cornea and crystalline lens remain transparent, allowing light to reach the retina with minimal scattering. Local or diffuse white or grey opacities may be detectable visually, due to structural abnormalities, inflammation, trauma or age-related degeneration, which leads to increased light scattering.

The impact of opacity-based disorders on a computer vision point of view is largely on the pixel intensity, local contrast, colour distribution and texture in the affected area. Thus, the following brightness and opacity extent, whiteness, texture homogeneity and edge visibility features from images are valuable information for automated detection.

Cataract is a progressive clouding of the crystalline lens caused by the accumulation of proteins that occurs with age, by congenital defects, metabolic diseases, or by eye trauma. As the transparency of the lens decreases, there is more intraocular light scattering, which causes blurring of vision, sensitivity to light glare, loss of contrast, and gradual vision loss. Cataracts in RGB photos are typically a greyish or whitish cloudiness that can be seen in the pupil, especially when they're more advanced. Thus, the detection of cataract typically depends on the intensity of the pupil, the distribution of opacity, variations in the texture and reflections of the pupil.

Sclerocornea is a rare congenital disease that causes the normally clear cornea to turn cloudy and look like that of the sclera. The line separating the cornea from the sclera becomes indistinct or even less distinct, resulting in a great loss of transparency of the cornea. Sclerocornea involves changes in the surface of the cornea as opposed to the lens, as is the case with cataracts. Thus, image-based detection is based on the evaluation of whiteness and visibility of the boundaries, opacification distribution and texture within the corneal area.

After traumatic injury, infection, inflammation, or previous corneal ulceration, corneal scarring occurs, resulting in fibrotic tissue in the cornea disrupting its transparency. The opacity may be very large, dense and located in different parts of the heart depending on the underlying disease. The characteristic appearance of a corneal scar in digital images is irregularly-shaped white to gray areas of heterogeneous appearance. Therefore, automated detection is based on the opacity localization, irregular texture, intensity variation, and morphology of the lesion.

Corneal Ulcer is an inflammatory condition where the corneal epithelium is lost and underlaid by stromal infiltration which is usually due to the microbial infection, trauma or severe dry eye. It can quickly get worse, and cause permanent vision loss if left untreated. Clinically, it exhibits symptoms of eye pain, redness, tearing, photophobia and blurred vision.

Corneal ulcers in RGB images are more likely to be whitish or yellowish with indistinct edges, and may or may not also have conjunctival hyperemia. In RGB images, corneal ulcers typically appear as localized whitish or yellowish opacities with irregular boundaries, often accompanied by conjunctival redness. An automated detection, from a computer vision point of view, is based on the analysis of the opacity, the morphology, the intensity distribution, the irregularity of the texture and the characteristics of the boundaries of the corneal area under the unconstrained imaging conditions of a webcam.

3.2. Shape Based

Shape-based disorders primarily affect the anatomical morphology of ocular structures while preserving tissue transparency. These abnormalities result in a change in the geometric structure of the iris or pupil and can therefore be detected by contour or shape features without colour or texture features.

Iris coloboma is a congenital developmental anomaly resulting from incomplete closure of the embryonic optic fissure. The condition results in an iris defect that is characterized as a keyhole or a teardrop shape, usually inferior to the pupil. Unlike opacity based disorders, iris coloboma does not affect the colour or brightness of the tissue, but rather it changes the contour of the pupil. Therefore, the focus on detection is on geometric properties like circularity, convexity, contour irregularity, radial distance signatures, and invariant shape descriptors.

3.3. Ring Appearance Based

Ring appearance-based disorders involve the development of a circular or annular (ring) formation around the iris. The abnormalities are mainly located in peripheral cornea and are best identified based on the colour, intensity, continuous and thickness of the abnormality and not on overall eye geometry.

Arcus senilis is a phenomenon associated with ageing, in which the peripheral corneal stroma contains lipid deposits giving rise to a greyish-white ring around the iris. While usually harmless in older people, it can happen in childhood and be a sign of systemic lipid metabolic diseases. Automated detection will be most effective if normalized annular areas around the iris are analyzed based on the ring continuity, thickness, intensity, radial intensity profile and colour distribution, since the lesion appears as a continuous peripheral ring.

3.4. Position Based

Positional disorders are abnormal eye alignment without necessarily affecting the eye anatomy or transparency. Such conditions primarily alter the relative positions of the pupils or visual axes and are therefore analyzed using geometric relationships derived from facial landmarks.

Squint, also known as strabismus. It is a binocular vision problem in which the visual axes of both eyes don't point in the same direction. The eye may turn in or out, up or down, and the other eye remains focused. It causes a lack of binocular vision and depth perception. In computer Vision, squint is typically detected by analyzing the relative position of the iris or pupil with respect to eyelid landmarks and eye corners. Landmark-based geometric measurements and symmetry analysis provide reliable indicators of ocular misalignment.

4. Proposed Methodology

This study proposes a non-invasive, webcam-based framework for detecting selected anterior eye abnormalities. It also generates personalized accessibility recommendations. The RGB video captured from a common laptop webcam is processed by using Media-Pipe Face Mesh for facial and ocular landmark localization, followed by visual analysis of the specific disease. The proposed framework involves five major steps: “video acquisition and eye landmark localization”, “disease-specific visual analysis”, “integration of features and generation of decisions”, “accessibility-profile generation”, and “personalized web-interface adaptation”. The framework classifies the abnormalities of the eye based on the dominant visual characteristics of the eye: position, opacity, shape, and ring appearance.

4.1. Face and Eye Landmark Detection

The input video is recorded from the regular laptop webcam and is processed one frame at a time. Media-Pipe Face Mesh is employed to estimate 478 three-dimensional facial landmarks. It allows for the localization of the eye contours, the boundaries of the iris and the centre of the pupil. These landmarks are used for the geometric references needed for later feature extraction of the diseases. The eye regions are normalized with respect to the eye geometry detected in order to minimize the effects of viewing distance, head pose and facial orientation on eye feature measurements. The result is then fed to the parallel disease-detection modules the landmark coordinates and the normalized eye regions. **Error! Unknown switch argument.** illustrates the facial, ocular, iris, and pupil landmark localization process.

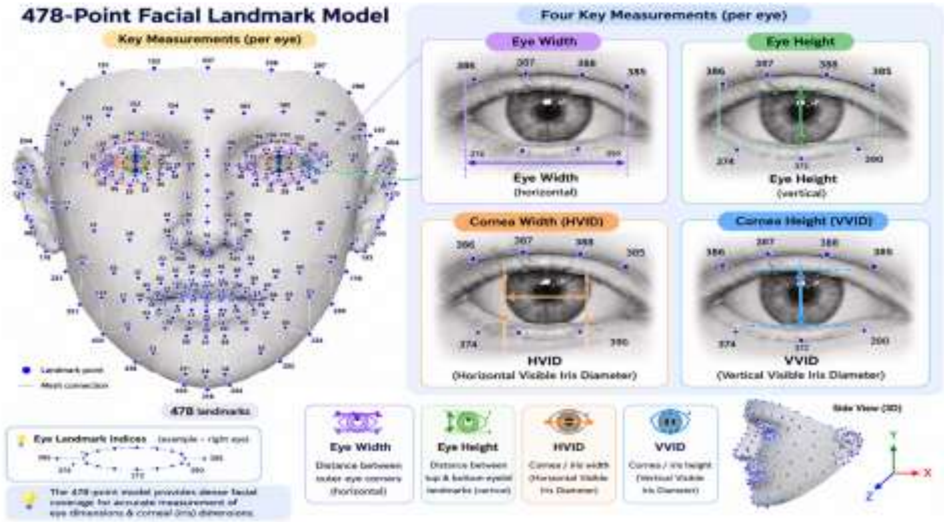

Figure 1: Media-Pipe facial landmark visualization

4.2. Position Based Impairedness detection

Position-based analysis is used to identify squint from the relative spatial configuration of the pupils. The method analyzes the position of each pupil with respect to anatomical eye landmarks obtained from the Media-Pipe Face Mesh. Based on the directional displacement of one or both pupils from their neutral positions, 17 ocular configurations are considered, comprising five normal configurations, eight unilateral-squint configurations, and four bilateral-squint configurations, as illustrated in **Error! Unknown switch argument.**.

For each frame, pupil positions are tracked using the corresponding iris and pupil landmarks. Geometric features describing the relative pupil position and ocular alignment are then extracted and evaluated against the predefined pupil-position configurations. This analysis enables identification of the 12 squint configurations, including unilateral and bilateral deviations, as illustrated in **Error! Unknown switch argument.**. The temporal consistency of the detected configuration can subsequently be used to improve the reliability of the final decision.

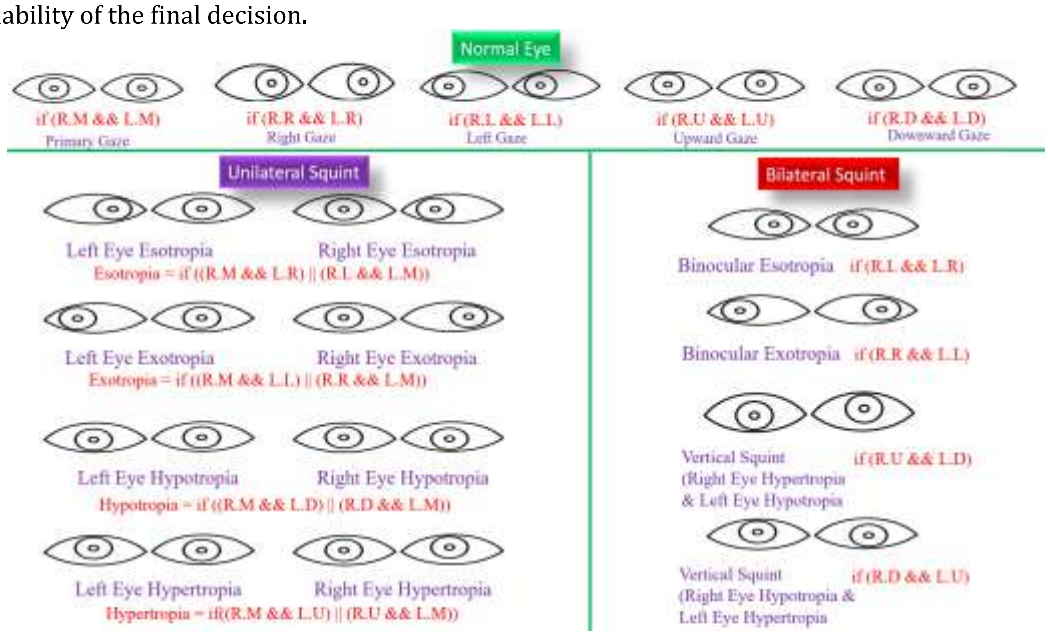

Figure 2: Positional alignments of pupil

4.3. Opaqueness Based Impairedness Detection

The opacity-based module analyzes cataract, sclerocornea, corneal scarring, and corneal ulcer according to intensity and structural characteristics observed within the pupil and corneal regions. The eye ROI is first converted to grayscale and processed using low-pass filtering and threshold-based analysis. The resulting intensity distribution is evaluated to identify opacity-related abnormalities.

The proposed decision sequence uses the experimentally defined pupil-intensity thresholds. When the measured pupil intensity is below 50, the eye is classified as normal according to the proposed criterion. An intensity between 50 and 100 indicates mild cataract. When the pupil intensity exceeds 100, the corneal region is further examined. If the increased intensity is primarily confined to the pupil, the condition is classified as severe cataract; if increased intensity extends across the corneal region, sclerocornea is considered.

Additional corneal analysis is performed to distinguish localized structural abnormalities. Localized fibrotic opacity is used as the characteristic indicator for corneal scarring, whereas active inflammatory lesion characteristics within the corneal region are used for corneal-ulcer detection. Thus, the opacity module provides disease-specific decisions for cataract, sclerocornea, corneal scarring, and corneal ulcer, as shown in **Error! Unknown switch argument.**.

4.4. Shape and Ring Appearance Based Detection

Iris coloboma is analyzed using pupil-shape characteristics. The pupil contour is extracted from the normalized eye ROI, followed by convex-hull and contour analysis. Shape descriptors, particularly circularity and deviations from the expected approximately circular pupil geometry, are used to identify abnormal pupil morphology. Non-circular configurations, including keyhole-, pear-, and oval-like contours, are considered candidate indicators of iris coloboma. The resulting shape features are evaluated to classify the eye as iris coloboma present or absent.

Arcus Senilis detection focuses on the characteristic whitish-gray peripheral corneal ring surrounding the iris. Following contrast enhancement using CLAHE, a peripheral corneal annular region is extracted using the detected iris geometry as the scale reference. This avoids dependence on a fixed pixel radius when the user's distance from the camera changes.

The annular region is analyzed to identify candidate whitish regions and determine whether they exhibit a ring-like spatial distribution. The principal features include normalized ring width, ring intensity, ring continuity, and radial position. The normalized ring width is measured relative to iris size, while ring intensity represents the intensity contrast between the candidate ring and the surrounding corneal region. Ring continuity and radial consistency are used to distinguish a circumferential/arcuate structure from isolated reflections or other bright regions. The final output is a binary decision: Arcus Senilis present or absent.

4.5. Overall Architecture

The complete framework operates on webcam video through a sequential acquisition and analysis pipeline. The input video is divided into individual frames, followed by user identification and facial landmark processing. For a new user, Media-Pipe Face Mesh is initialized and the ocular landmarks required for subsequent analysis are extracted. For a returning user, the previously generated accessibility profile can be activated directly, subject to the system's user-identification mechanism.

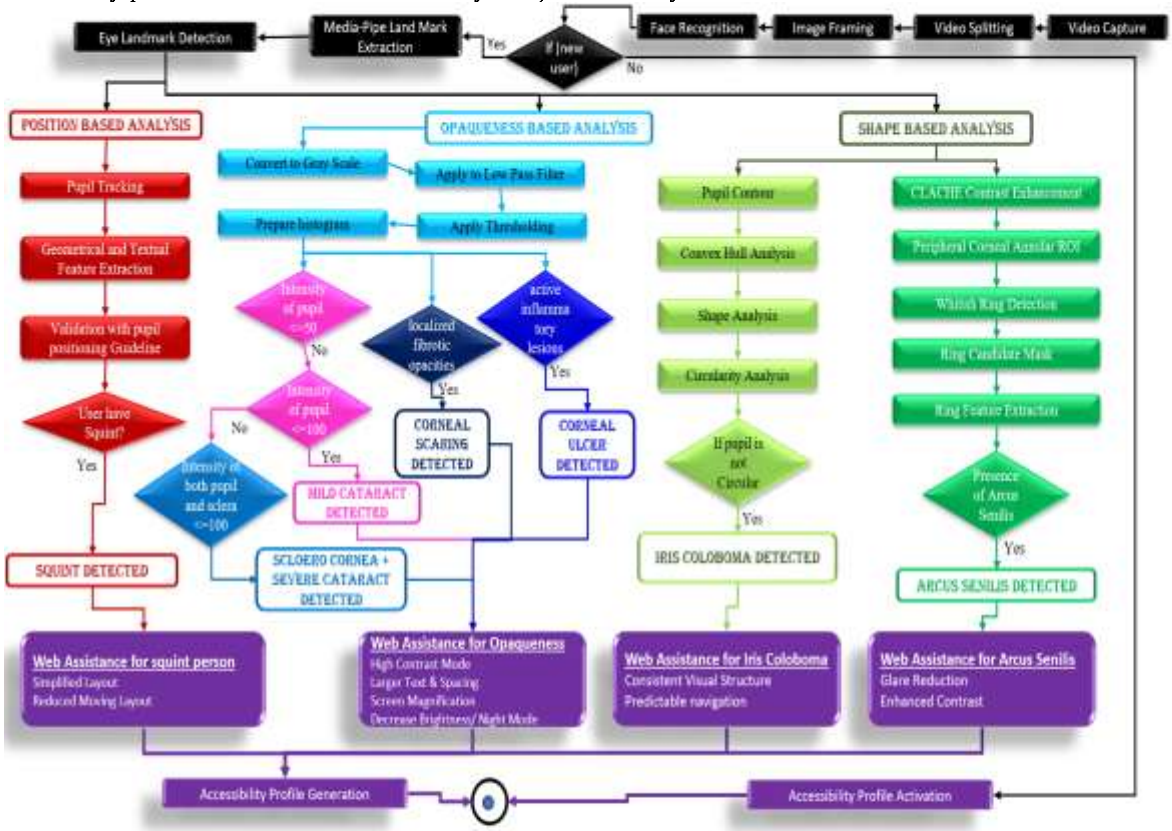

Figure 3: Overall Methodology

Following landmark localization, the position, opacity, shape, and ring-appearance-based modules operate in parallel. It allow different ocular characteristics to be analyzed independently. The resulting disease-specific decisions are integrated into a unified impairment profile covering the seven target conditions: squint, cataract, sclerocornea, corneal scarring, corneal ulcer, iris coloboma, and Arcus Senilis.
Rather than relying on a single generic feature representation, the framework combines complementary geometric, intensity, structural, and appearance-based evidence obtained from the corresponding disease modules. The integrated output is then forwarded to the accessibility layer for profile generation and interface adaptation. The complete processing architecture is presented in **Error! Unknown switch argument.**.
The detected impairment profile is translated into personalized accessibility requirements through a disease-to-accessibility mapping mechanism. Instead of presenting only the detected ocular condition, the system uses the impairment profile to determine appropriate web-interface adaptations. Examples include increased text size, enhanced contrast, magnification, simplified layouts, reduced visual clutter, improved spacing, and focus/navigation assistance.
For example, opacity-related impairments may benefit from enhanced contrast, larger text, and magnification, whereas position-related impairment may benefit from simplified layouts, reduced visual distraction, and clearly distinguishable interactive elements. The resulting adaptations are stored as a user-specific accessibility profile.
For a returning user, the stored accessibility profile can be activated to automatically configure the web interface according to the previously established requirements. For a new user, the detected impairment profile is used to generate the initial accessibility configuration. This mechanism allows the proposed framework to connect ocular-condition detection with personalized human–computer interaction rather than limiting the system to disease classification alone.

4.6. Dataset Description

Publicly available ocular datasets predominantly contain high-resolution clinical images acquired using specialized ophthalmic equipment under controlled conditions. Such datasets do not directly represent the appearance of users captured through laptop webcams and are therefore not fully aligned with the proposed accessibility-oriented application. Accordingly, a hybrid dataset comprising clinical ocular samples and webcam-acquired facial videos was constructed for this study.
The dataset contains 1,000 video samples distributed across eight classes: Squint (200), Cataract (200), Sclerocornea (50), Corneal Scarring (50), Corneal Ulcer (50), Iris Coloboma (100), Arcus Senilis (100), and Normal (250). Impaired-eye samples were collected from Naitrika Eye Care, Berhampur, and Red Cross Blind School, Berhampur, between February and April 2026. Normal-vision samples were obtained from volunteers at Parala Maharaja Engineering College and Berhampur University during the same period.
Before data acquisition, participants were informed about the study objectives, data-collection procedures, and intended research use. Written informed consent was obtained from adult participants, while parental or legal-guardian consent and participant assent were obtained where applicable for participants below 18 years of age. Participant confidentiality was maintained throughout data acquisition, storage, and analysis.
All recordings were obtained using standard laptop webcams under controlled illumination. Each video has an average duration of approximately 10 seconds and contains frontal facial views suitable for frame-wise ocular analysis. Participants ranged from 16 to 65 years, providing variation in age, facial characteristics, and acquisition conditions. This variability is intended to improve the practical robustness and generalization of the proposed webcam-based framework.

4.7. Implementation Details

The proposed framework was implemented in Python for real-time webcam-based ocular assessment and accessibility-aware web personalization. OpenCV was used for video acquisition, frame extraction, and image preprocessing, while Media-Pipe Face Mesh was employed for facial, ocular, iris, and pupil landmark localization. NumPy and SciPy were used for geometric measurements, feature extraction, and numerical/statistical operations.
Experiments were conducted on lenovo laptop equipped with an Intel Core i5 processor (13 Generation), 8 GB RAM, 4 GB GPU, and an integrated 1 MP webcam. The framework is designed to operate on commodity computing hardware without requiring dedicated ophthalmic imaging equipment. This architecture supports potential deployment as a browser- or web-application-based accessibility system. Representative detection outputs of the proposed framework are presented in **Error! Unknown switch argument.**

Figure 4: Model's results for some users

5. Result Analysis

The proposed framework was evaluated on a held-out test set of 1,000 samples covering seven ocular conditions (viz. Squint, Cataract, Sclerocornea, Corneal Scarring, Corneal Ulcer, Iris Coloboma, and Arcus Senilis) along with the Normal class. The evaluation considered classification performance, comparative characteristics, accessibility adaptation, feature ablation, and system limitations.

5.1. Performance

This The confusion matrix shows that 982 of 1,000 samples were correctly classified, yielding an overall accuracy of 98.20% and a misclassification rate of 1.80%. The model achieved a Macro-F1 score of 0.9763 and a Weighted-F1 score of 0.9820, indicating consistently strong performance across classes despite unequal class distributions. **Error! Unknown switch argument.** represents the 8x8 class confusion Matrix.

Class-wise Precision for squint, Cataract, Sclero-Cornea, Corneal Scaring, Corneal-Ulcer, Iris Coloboma, Arcus Senilis, normal is 100%, 97.49%, 92.59%, 100%, 95.83%, 100%, 100%, 97.28% respectively. Similarly class-wise Recall for squint, Cataract, Sclero-Cornea, Corneal Scaring, Corneal-Ulcer, Iris Coloboma, Arcus Senilis, normal is 98.50%, 97.00%, 100%, 94.00%, 92.00%, 100%, 98.00%, and 100% respectively. The proposed model achieved highest precision for squint, corneal scaring, Iris coloboma, normal detection. Similarly the model achieved highest recall for Sclerocornea, Iris Coloboma, and Normal detection. The model also maintained high specificity for four classes. The results demonstrate that the proposed feature representation can effectively discriminate multiple ocular conditions from webcam-acquired visual information. The observed errors are limited to a small number of visually related class combinations.

The confusion matrix shows that the majority of classification errors occur between classes having potentially similar visual manifestations. In particular, cataract is confused with corneal scarring, corneal ulcer, and sclerocornea. The 18 total classification errors are distributed across a limited number of class pairs rather than being uniformly distributed across all classes. This is important because it indicates that the framework has learned highly discriminative representations for several conditions, while the remaining errors are concentrated in visually similar categories.

Figure 5: 8 X 8 class confusion matrix

5.2. Comparative Analysis

Existing ocular-disease detection systems predominantly utilize clinical, slit-lamp, fundus, near-infrared, or AS-OCT images combined with machine learning or deep learning techniques. Although these approaches can achieve high diagnostic accuracy, their deployment generally requires specialized imaging equipment, controlled acquisition environments, and clinical expertise, limiting their applicability in everyday computing settings.

In contrast, the proposed framework analyses RGB webcam video using Media-Pipe Face Mesh to localize facial, ocular, iris, and pupil landmarks. Disease-specific visual descriptors are then applied across four analytical categories (viz. position, opacity, shape, and ring appearance) to identify squint, cataract, sclerocornea, corneal scarring, corneal ulcer, iris coloboma, and Arcus Senilis. Scale-normalized measurements reduce sensitivity to user-to-camera distance and head orientation, while contour, intensity, and appearance features characterize disease-specific abnormalities.

A further distinction is the integration of ocular screening with accessibility-aware personalization. Instead of terminating at disease classification, the proposed system generates an impairment profile that can drive interface adaptations such as text enlargement, contrast enhancement, magnification, spacing optimization, simplified layouts, and navigation support.

On the evaluated test set, the framework achieved 98.20% accuracy, demonstrating its feasibility for multi-class ocular-condition screening. **Error! Unknown switch argument.** summarizes the principal differences between existing approaches and the proposed framework.

Table 1: Comparative Analysis of proposed system with existing models

Reference	Application	Accuracy	Personalised Accessibility support for web access
Ref [1] to [5]	Six type of Squint Detection from image	90% to 98%	
Ref [6]	Squint and Cataract detection from live laptop camera videos	98.39% and 96.90% for squint and cataract detection respectively	Yes
Ref [10]	Iris Coloboma Detection detection from Retinal Image	96%	
Ref [12] to [17]	Arcus Senilis Detection	95% to 96%	
Ref [18] to [23]	Cataract detection from fundus image or high resolution near infrared eye image	96% to 99% from retinal images 96% to 97% from near infrared eye images images	
Ref [32] to [34]	Corneal Ulcer Detection	94% to 98%	
Proposed Model	Detection of seven type of impairedness (Squint, Cataract, Sclero-Cornea, Corneal Scaring, Corneal Ulcer, Iris Coloboma, Arcus Senilis) detection from live videos	overall accuracy 98.02%	Yes

5.3. Limitation

The proposed framework demonstrates promising performance but has several limitations. The current implementation assumes a single frontal user, and facial landmark localization may become unreliable in the presence of multiple faces, substantial head rotation, or facial occlusion. Detection performance is also influenced by image quality, illumination, camera resolution, reflections, image noise, and user-to-camera distance, which can affect ocular feature extraction. Experimental observations indicate that a minimum camera resolution of approximately 1 MP is required for stable localization of iris and pupil landmarks. Lower-resolution images may reduce the reliability of ocular measurements and consequently affect impairment classification. In addition, visually similar conditions, particularly cataract, sclerocornea, corneal scarring, and corneal ulcer, remain comparatively difficult to distinguish using standard RGB webcam images.

6. Conclusion

This study presented a webcam-based framework for automated detection of visually observable ocular impairments and accessibility-aware web personalization. The proposed system employs MediaPipe Face Mesh for real-time facial and ocular landmark localization and analyzes disease-specific characteristics through four complementary categories: position, opacity, shape, and ring appearance. These modules enable detection of squint, cataract, sclerocornea, corneal scarring, corneal ulcer, iris coloboma, and Arcus Senilis using RGB images acquired from a standard laptop webcam.

Evaluation on the 1,000-sample test set achieved an overall classification accuracy of 98.20%, demonstrating the feasibility of the proposed multi-condition screening approach. The framework also incorporates scale-normalized ocular measurements to reduce the influence of variable user-to-camera distance and integrates the detected impairment profile with an accessibility recommendation engine for personalized web-interface adaptation.

Future work will focus on developing a browser-integrated plugin capable of automatically generating personalized accessible web interfaces for users with visual or hearing impairments based on their detected accessibility requirements.

Acknowledgment

The authors sincerely acknowledge the CSE Department of Parala Maharaja Engineering College, for providing access to the PARAM SHAVAK High-Performance Computing (HPC) Laboratory and the computational infrastructure required for conducting the experimental evaluations. The authors also gratefully acknowledge Dr. Aswini Behera, Ophthalmologist at Niatrika Eye Hospital, for providing valuable clinical guidance and expert insights into the ocular characteristics and medical features considered in this study.

Declarations (Heading 5)

Author contribution. A. R. Dash and M. R. Patra contributed equally to the development of the proposed model and the writing of the research paper.

Funding statement. The authors declare that they have not received any funding or financial support from any institution or funding agency for this research.

Conflict of interest. The authors declare no conflict of interest.

Availability of Data and Materials. The datasets generated and analyzed during the current study are available from the corresponding author on reasonable request.

Informed Consent. Written informed consent was obtained from all participants prior to data collection after explaining the purpose of the study, the nature of the data being collected, and its intended use for research.

References

1. M. Yarkheir, M. Sadeghi, H. Azarnoush, M. R. Akbari, and E. Khalili Pour, (2025). "Automated strabismus detection and classification using deep learning analysis of facial images". Scientific Reports, Vol. 15(1), 3910, https://doi.org/10.1038/s41598-025-88154-6.
2. D. Wu, Y. Li, H. Zhang, X. Yang, Y., Mao, B. Chen, Y. Feng, L. Chen, X. Zou, Y. Nie, T. Yin, Z. Yang, J. Liu, W. Shang, G. Yang, and L. Liu, (2024). "An artificial intelligence platform for the screening and managing of strabismus". Eye, Vol. 38(16), pp 3101-3107, https://doi.org/10.1038/s41433-024-03228-5.
3. W. Kurdthongmee, L. Udomvej, A. Sukkuea, P. Kurdthongmee, C. Sangeamwong, and C. Chanakarn, (2024). "Strabismus Detection in Monocular Eye Images for Telemedicine Applications". Journal of Imaging, Vol. 10(11), 284, pp1-18, https://doi.org/10.3390/jimaging10110284.
4. S. Joshi, (2025). "Advanced CNN Approach To Automated Squint Eye Detection And Comprehensive Early Intervention". Journal of Scientific Research and Technology, vol. 3(7), pp 131-145.
5. S. Karaaslan, S. G. Kobat, and M. Gedikpınar, (2023). "A new method based on deep learning and image processing for detection of strabismus with the Hirschberg test", Photodiagnosis and Photodynamic Therapy, Vol. 44, 103805, pp 1-12, https://doi.org/10.1016/j.pdpdt.2023.103805.
6. A. R. Dash, and M. R. Patra, (2026). "Video-Based Detection of squint and cataract for accessibility-aware adaptive web interface rendering". arXiv preprint arXiv:2607.07099.
7. B. O. Adegoke, E. O. Omidiora, S. A., Falohun, and J. A. Ojo, (2013). "Iris Segmentation: a survey". International Journal of Modern Engineering Research (IJMER), Vol. 3(4), pp. 1885-1889.
8. Z. Liu, Y., Chen, Z., Lin, X. and Shi, (2017). "Ophthalmic clues to the endocrine disorders". Journal of

Endocrinological Investigation, Vol. 40(1), pp. 21-25, DOI: 10.1007/s40618-016-0532-7.
9. J. Daugman, (2007). "New methods in iris recognition". IEEE Transactions on Systems, Man, and Cybernetics, Part B (Cybernetics), Vol. 37(5), pp. 1167-1175, DOI: 10.1109/TSMCB.2007.903540.
10. C. Pratibha, and K. Yalagi, (2025, November). "Automated Detection of Eye Coloboma using ,Vision Transformers and Explainable AI Techniques". In 2025 IEEE 7th International Conference on Computing, Communication and Automation (ICCCA), IEEE, pp. 1-6, DOI: 10.1109/ICCCA66364.2025.11325176.
11. G. Z. Armstrong, K. K. Ho, T. J., Knight, and E. E. Conboy, (2025). "Novel Variant of RARB Gene in Familial Isolated Ocular Coloboma: A Case Report". The American Journal of Case Reports, 26, e949311.
12. R. A. Ramlee, K. Azha, and R. S. S. Singh, S. (2011). "Detecting cholesterol presence with iris recognition algorithm". Biometric Systems, Design and Applications, 129-149.
13. S. G. Songire, and M. S. Joshi, (2016). "Automated detection of cholesterol presence using iris recognition algorithm". International Journal of Computer Applications, Vol. 133(6), pp. 41-45.
14. V. Bhangdiya, (2014). "Cholesterol presence detection using iris recognition". Vol. 1(2), pp1-4.
15. R. A. Ramlee, K. A. Aziz, S. Ranjit, and M. Esro, (2011). "Automated detecting arcus senilis, symptom for cholesterol presence using iris recognition algorithm". Journal of Telecommunication, Electronic and Computer Engineering (JTEC), Vol. 3(2), pp. 29-39.
16. M. K. SV, G. R, (2018). "Computer-aided diagnosis of anterior segment eye abnormalities using visible wavelength image analysis based machine learning". Journal of medical systems, Springer, Vol. 42(7), 128 pp. 1-12.
17. N. Amini, and A. Ameri, (2020). "A deep learning approach to automatic recognition of arcus senilis". Journal of biomedical physics & engineering, Vol. 10(4), pp. 507-512.
18. M. Yang, J. J. Yang, Q. Zhang, Y. Niu, and J. Li, (2013, October). "Classification of retinal image for automatic cataract detection", In 2013 IEEE 15th International Con-ference on e-Health Networking, Applications and Services (Healthcom 2013), pp. 674-679, DOI: 10.1109/HealthCom.2013.6720761.
19. M. S. Junayed, M. B. Islam, A. Sadeghzadeh, and S. Rahman, (2021). "CataractNet: An automated cataract detection system using deep learning for fundus images", IEEE ac-cess, 9, pp 128799-128808.
20. I. Khan, W. Akbar, A. Soomro, T. Hussain, I. Khalil, M. N., Khan, and A. Salam, (2024). "Enhancing ocular health precision: Cataract detection using fundus images and ResNet-50". ICCK Transactions on Intelligent Systematics, Vol. 1(3), pp 145-160, DOI: 10.62762/TIS.2024.640345.
21. H. Wu, J. Lv, and J. Wang, (2021, July). "Automatic cataract detection with multi-task learning". In 2021 International Joint Conference on Neural Networks (IJCNN), IEEE, pp. 1-8, 10.1109/IJCNN52387.2021.9533424.
22. P. Tripathi, Y. Akhter, M. Khurshid, A. Lakra, R. Keshari, M. Vatsa, and R. Singh, (2022). "MTCD: Cataract detection via near infrared eye images", Computer Vision and Image Understanding, 214, 103303, pp 1-10, https://doi.org/10.1016/j.cviu.2021.103303.
23. T. Ganokratanaa, M. Ketcham, and P. Pramkeaw, (2023). "Advancements in cataract detection: The systematic development of LeNet-convolutional neural network models". Journal of Imaging, Vol. 9(10), 197, pp 129, https://doi.org/10.3390/jimaging9100197
24. N. Gupta, A. Varshney, M. Ramappa, S. Basu, V. Romano, M. Acharya, A. Gaur, N. Kapur, A. Singh, G. Shah, I. Chauchary, N. Patel, A. Tiwari, A. Kale, V. Sangwan, and U. Mathur, (2022). "Role of AS-OCT in managing corneal disorders". Diagnostics, Vol. 12(4), 918, pp. 1-17, DOI: 10.3390/diagnostics12040918. .
25. A. M. Rollins, M. V. Sivak, S. Radhakrishnan, J. H. Lass, D. Huang, K. D., Cooper, and J. A. Izatt, (2002). "Emerging clinical applications of optical coherence tomography". Optics and Photonics News, Vol. 13(4), pp. 36-41.
26. S. Radhakrishnan, A. M. Rollins, J. E. Roth, S., Yazdanfar, V., Westphal, D. S. Bardenstein, and J. A. Izatt, (2001). "Real-time optical coherence tomography of the anterior segment at 1310 nm". Archives of ophthalmology, Vol. 119(8), pp. 1179-1185, DOI: 10.1001/archopht.119.8.1179.
27. Y. Ueno, H. Mori, K. Kikuchi, M., Yamanari, and T. Oshika, (2021). "Visualization of anterior chamber angle structures with scattering-and polarization-sensitive anterior segment optical coherence tomography". Translational vision science & technology, Vol. 10(14), 29-29, DOI: 10.1167/tvst.10.14.29.
28. M. Lombardo, M. Parekh, S. Serrao, A. Ruzza, S. Ferrari, and G. Lombardo, (2017). "Two-photon optical microscopy imaging of endothelial keratoplasty grafts". Graefe's Archive for Clinical and Experimental Ophthalmology, Vol. 255(3), ppp. 575-582, DOI: 10.1007/s00417-016-3543-3.
29. M. J. A. Girard, M. Ang, C. W. Chung, M. Farook, N. Strouthidis, J. S. Mehta, and J. M. Mari, (2015). "Enhancement of corneal visibility in optical coherence tomography images using corneal adaptive compensation". Translational vision science & technology, Vol. 4(3), 3-3, pp. 1-11, DOI: /10.1167/tvst.4.3.3.
30. J. L. Simpson, C. J. Nien, K. J. Flynn, J. V. Jester. (2011). "Evaluation of topical cysteamine therapy in the CTNS(-/-) knockout mouse using in vivo confocal microscopy". Mol Vis. 2011;17:2649-54. Epub 2011

Oct 8. PMID: 22065917; PMCID: PMC3209421.
31. M. J. Cree, and H. F. Jelinek, (2008, February). "The effect of JPEG compression on automated detection of microaneurysms in retinal images". In Image Processing: Machine Vision Applications (Vol. 6813, pp. 180-189). SPIE.
32. I. A. Qasmieh, H. Alquran, A. A. Zyout, Y. Al-Issa, W. A. Mustafa, and M. Alsalatie, (2022). "Automated detection of corneal ulcer using combination image processing and deep learning". Diagnostics, Vol. 12(12), 3204, pp. 1-20, DOI: 10.3390/diagnostics12123204.
33. D. Manawongsakul, and K. Patanukhom, (2024). "A segmentation-based automated corneal ulcer grading system for ocular staining images using deep learning and hough circle transform". Algorithms, Vol. 17(9), 405, pp 1-28, 10.3390/a17090405.
34. T. B. Alakuş, and M. Baykara, (2024). "Classification and Determination of Severity of Corneal Ulcer with Vision Transformer Based on the Analysis of Public Image Dataset of Fluorescein-Stained Corneas". Diagnostics, Vol. 14(8), 786, pp. 1-20, DOI: 10.3390/diagnostics14080786.
35. H. M. S. C. Herath, T. H. M. P. Swarnajith, W. S. H. M. Senanayaka, , H. W. R. A. Hettiarachchi, N. Walgampaya, and R. D. Zoysa (2025, December). "Eye Health Monitoring and Eye Care System". In 2025 7th International Conference on Advancements in Computing (ICAC), IEEE, pp. 1-6, DOI: 10.1109/ICAC69156.2025.11361466
36. Y. Kartynnik, A. Ablavatski, I. Grishchenko, and M. Grundmann, (2019). "Real-time facial surface geometry from monocular video on mobile GPUs". arXiv preprint arXiv:1907.06724.
37. M. R. Patra, A. R. Dash, and P. K. Mishra, (2017). "A quantitative analysis of WCAG 2.0 compliance for some Indian web portals", International Journal of Computer Science, Engineering and Application (IJCSEA), AIRCC, Vol. 4(1), PP. 9-24, DOI: 10.5121/ijcsea.2014.4102, arXiv preprint arXiv:1710.08788.
38. M. R. Patra, A. R. Dash, and P. K. Mishra, (2014, October). "Accessibility analysis of government web portals of Asian countries". In Proceedings of the 8th International Conference on Theory and Practice of Electronic Governance, ACM, pp. 383-386, DOI: 10.1145/2691195.2691253.
39. M. R. Patra, and A. R. Dash, (2017). "Accessibility analysis of web browsers". International Journal of Services Technology and Management, Inder-science, Vol. 23(4), PP. 313-330, DOI: 10.1504/IJSTM.2017.088161.
40. M. R. Patra, and A. R. Dash, (2017, March). "Analysis of Android Cell Phone Web-Browsers to Facilitate Accessible m-Governance". In Proceedings of the 10th International Conference on Theory and Practice of Electronic Governance, ACM (pp. 276-284).